

Stability of Thermocapillary Convection in the Float-Zone Process for the Manufacturing of Semiconductor Crystals

Hans D. Mittelmann
Arizona State University
Department of Mathematics
P.O. Box 871804
Tempe, AZ 85287-1804, USA

March 28, 1996

Abstract

Some of the most challenging eigenvalue problems arise in the stability analysis of solutions to parameter-dependent nonlinear partial differential equations. Surface tension gradients along the free boundary of the float-zone in crystal growth give rise to a stationary thermocapillary convection. Loss of stability leads to undesirable material imperfections. Stability analyses employing both energy and linearized theory are employed. In each case complex, large, and sparse generalized eigenvalue problems have to be solved. Methods for their solution are proposed and the numerical results are compared to experimental results.

1 Introduction

The float-zone crystal-growth process is a containerless method for producing high-quality electronic material in which a rod of the material to be refined is passed through a type of heater, producing a zone of molten material that is held in place by surface-tension forces, cf. Figure 1. The requirement that surface-tension forces alone support the weight of the molten zone makes the process unsuited for use with certain materials (notably gallium arsenide) in terrestrial environments. Consequently, there has been a great deal of interest in exploring the microgravity environment of space to grow larger crystals of electronic material using the float-zone method [7, 24, 29].

Along with the reduction in weight provided by a microgravity environment comes a reduction in any convection in the melt induced by buoyancy. At one time, it was believed that buoyancy induced convection was responsible for the appearance of *striations* observed in float-zone-grown material. If this were the case, then one might also expect to produce *better* material in a microgravity environment. Associated with the float-zone process, however, is another type of convection which will not vanish in space, namely *thermocapillary convection*, driven by temperature-induced surface-tension gradients along the free surface of the melt, cf. Figure 2.

In fact, it has been widely speculated that the *instability* of this convective mode is responsible for the appearance of the observed *striations*. The desire to utilize the unique environment of space coupled with these observations has led to a significant body of research associated with the stability of thermocapillary convection in models of the float-zone process.

Hydrodynamic stability theory is concerned with determining the conditions under which a certain flow, called the *basic state*, will remain stable or become unstable due to the inevitable presence of unknown perturbations. In general, these perturbations are governed by nonlinear partial differential equations. For a general reference on stability theory we refer to [9]. Linear-stability theory assumes the perturbations to be infinitesimally small and neglects the nonlinear terms in comparison with their linear counterparts. This theory is local in nature and results in a criterion which guarantees growth

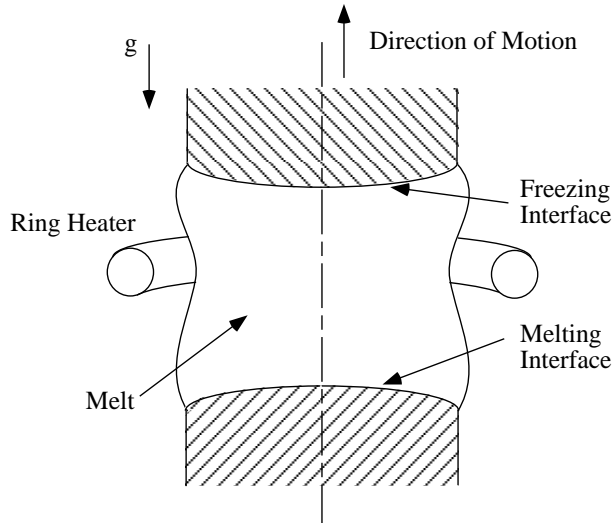


Figure 1: The float-zone crystal growth process

of these small disturbances. Typically, an externally controllable dimensionless parameter, say R , is selected and linear theory yields a value R_L such that $R > R_L$ is a sufficient condition for instability.

Energy stability theory, on the other hand, adopts a global approach by examining the behavior of a generalized integral disturbance-energy. Unlike linear stability theory, energy-stability theory provides a value R_E such that $R < R_E$ is a sufficient condition for stability of a given basic state to disturbances of *arbitrary amplitude*. This technique is equivalent to a stability analysis utilizing a Lyapunov function. The application of either theory gives rise, in general, to an eigenvalue problem.

If R_E and R_L should coincide, a rigorous stability bound is obtained. However, this is usually not the case and the proximity of R_E to R_L is a function of the physical mechanism that gives rise to the instability. Two such mechanisms for which R_E and R_L may be expected to be relatively close to each other are buoyancy and thermocapillarity.

Experimentally, it has been shown by Preisser, Schwabe and Scharmann [23], among others, that thermocapillary convection in a model of the float-zone process undergoes a transition from steady to oscillatory convection when a dimensionless parameter known as the *Marangoni number* exceeds a particular value, the other parameters held fixed. The geometry employed by Preisser et al. is termed a *half-zone* because it is meant to simulate the lower half of an actual float-zone. It consists of a pair of coaxial, solid cylindrical rods, oriented vertically, with a bridge of liquid material suspended between them. The rods are heated differentially, with the upper rod being at a higher temperature than the lower one. Buoyancy, therefore, plays a stabilizing role in the experiment since the liquid is stably stratified due to temperature in the axial direction. The basic state of thermocapillary convection that results consists of a single toroidal eddy with motion on the free surface in the direction from the hot cylinder toward the cold one.

Motivated by the above work, Shen et al. [26] undertook a stability analysis of a half-zone of $O(1)$ aspect ratio, employing energy-stability theory rather than linear theory. Their results, computed primarily for Prandtl number $Pr = 1$, compared favorably with the experimental results of Preisser et al. However, their analysis had made the simplifying assumption of permitting only axisymmetric disturbances, while the oscillations observed by Preisser et al. were clearly *nonaxisymmetric* and for a material with significantly larger Prandtl number.

Computations for general disturbances were undertaken by Neitzel et al. [20]. The numerical method is described in [16]. Fortunately, experiments performed by Velten, Schwabe and Scharmann [28] for *KCl* provided results for unit Prandtl numbers that eliminated the need to attempt the more difficult calculations for larger Prandtl numbers. These newer energy-theory results are in excellent agreement with the experimentally determined onset Marangoni numbers in order of magnitude, al-

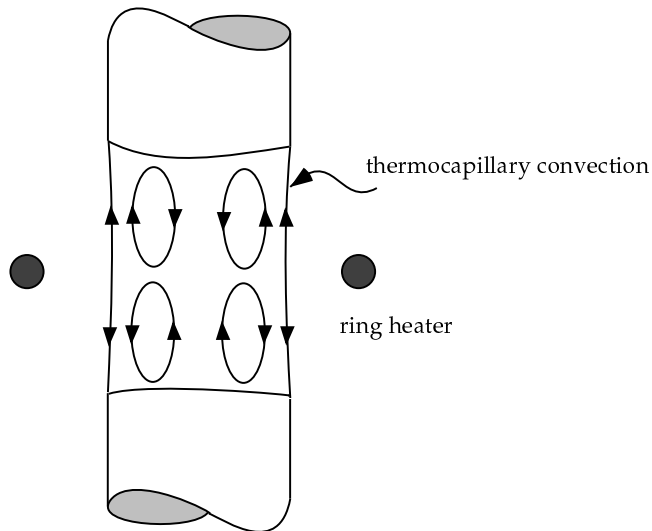


Figure 2: Thermocapillary convection in the float-zone

though the azimuthal structure emerging from the energy theory does not (and should not necessarily) agree with that observed experimentally.

The paper [19] completed the stability picture for the finite half-zone with a non-deformable free surface by calculating linear-stability limits for this basic state. The numerical method is described in [15]. The degree of closeness of the linear- and energy-theory results provides a bound for the region of parameter space *possibly* subject to nonlinear instability. The results show that the energy bound is less than the linear bound, but both are of the same order. The result would be consistent with subcritical Hopf bifurcation. To determine if, in fact, this is the case, additional computations would have to be done (cf. [9]). This may be done in future work. Since, furthermore, both bounds do not correspond to axisymmetric modes, *symmetry* of the basic state appears to be *broken*.

In this paper for the first time both the energy and linear approaches are outlined and exemplary numerical results are quoted. For other recent work on this subject, see, for example, [12, 13, 14].

2 Basic state

The basic state of interest is one of swirl-free thermocapillary convection in a model half-zone of $O(1)$ aspect ratio. The flow and temperature fields are two-dimensional and must therefore be obtained numerically for the nonlinear cases of interest. We model the liquid zone as a Newtonian, Boussinesq fluid and choose scales for length, velocity and pressure to be R , $\gamma(T_H - T_C)/\mu$, and $\gamma(T_H - T_C)/R$, respectively. The quantity μ is the dynamic viscosity coefficient and $\gamma > 0$ is the rate of decrease of surface tension σ with temperature, as defined by $\sigma = \sigma_m - \gamma(T - T_m)$, where $T_m = \frac{1}{2}(T_H + T_C)$ is the mean temperature of the two solid cylinders and σ_m is the surface tension at temperature T_m . The velocity scale is the Marangoni velocity obtained by balancing the surface-tension gradient along the interface with the jump in shear stress. A dimensionless temperature is defined by

$$\Theta \equiv \frac{T - T_m}{T_H - T_C}.$$

The resulting dimensionless governing equations for the velocity $\mathbf{U} \equiv (U, V, W)$, pressure P and temperature fields are

$$\frac{1}{r}(rU)_r + \frac{1}{r}V_\theta + W_z = 0, \quad (2.1)$$

$$\text{Re} \left(UU_r + \frac{1}{r} VU_\theta + WU_z \right) - \frac{1}{r} V^2 = -P_r + \nabla^2 U - \frac{U}{r^2} - \frac{2}{r^2} V\theta, \quad (2.2)$$

$$\text{Re} \left(UV_r + \frac{1}{r} VV_\theta + WV_z \right) + \frac{1}{r} UV = -\frac{1}{r} P_\theta + \nabla^2 V - \frac{V}{r^2} + \frac{2}{r^2} U\theta \quad (2.3)$$

$$\text{Re} \left(UW_r + \frac{1}{r} VW_\theta + WW_z \right) = -P_z + \nabla^2 W + \frac{Gr}{Re} \Theta, \quad (2.4)$$

$$Ma \left(U\Theta_r + \frac{1}{r} V\Theta_\theta + W\Theta_z \right) = \nabla^2 \Theta, \quad (2.5)$$

where

$$\nabla^2 \equiv \frac{1}{r} \frac{\partial}{\partial r} \left(r \frac{\partial}{\partial r} \right) + \frac{1}{r^2} \frac{\partial^2}{\partial \theta^2} + \frac{\partial^2}{\partial z^2}.$$

The basic state velocity of the axisymmetric basic state satisfies (2.1), (2.2), (2.4), (2.5) with all terms involving V , θ omitted. The three dimensionless parameters which appear are:

$$\text{Reynolds number} \quad \text{Re} = \frac{\gamma(T_H - T_C)R}{\mu\nu},$$

$$\text{Grashoff number} \quad \text{Gr} = \frac{g\alpha(T_H - T_C)R^3}{\nu^2},$$

$$\text{Marangoni number} \quad \text{Ma} = \frac{\gamma(T_H - T_C)R}{\mu\kappa},$$

where g is the gravitational acceleration, α is the coefficient of volumetric expansion and the conventional subscript notation has been used to denote partial differentiation. The Prandtl number is obtained from the quotient Ma/Re .

We assume, as a first approximation, that the free surface is not permitted to deform, and so is fixed at $r = 1$. This corresponds to requiring that the volume of liquid in the half zone is $\pi\Gamma$ and that the mean surface tension, σ_m , is asymptotically large. The boundary conditions applied to complete the problem specification are:

$$U = W = 0 \quad , \quad \Theta = -\frac{1}{2}; \quad z = 0 \quad (2.6)$$

$$U = W = 0 \quad , \quad \Theta = \frac{1}{2}; \quad z = \Gamma \quad (2.7)$$

$$U = 0, \quad U_z + W_r = -\Theta_z, \quad -P + 2U_r = \frac{-\sigma}{\sigma_m Ca}, \quad (2.8)$$

$$\Theta_r = \text{Bi}[\Theta - \Theta_a(z)]; \quad r = 1$$

$$U = W_r = \Theta_r = 0; \quad r = 0. \quad (2.9)$$

Equations (2.6) and (2.7) express the kinematic and no-slip conditions and the requirement of isothermal surfaces, while (2.8a) is the kinematic condition on the free surface. Equations (2.8b,c) represent the shear and normal-stress balances. Symmetry conditions at the axis of symmetry are given by (2.9). The additional parameter appearing in (2.8d), which models the heat-transfer mechanism at the free surface, is the Biot number, $\text{Bi} = hR/k$ where h is a heat-transfer coefficient and k is the thermal conductivity of the liquid. Since h may vary with z , in general, $\text{Bi} = \text{Bi}(z)$. This simple conductive mechanism for heat transfer between the liquid and the external environment (at specified temperature $\Theta_a(z)$) was adopted for consistency with the work of Xu and Davis [29]. For the majority of the calculations $\Theta_a(z) = -1/2$, i.e., the environment was assumed to be at a constant temperature equal to that of the cold cylinder at $z = 0$. Condition (2.8c) contains the capillary number $\text{Ca} = \gamma(T_H - T_C)/\sigma_m$ which vanishes in the limit of a non-deformable free-surface. Hence, this condition is not required in the present analysis.

The numerical solution of this problem is accomplished by first transforming the axisymmetric equations to a *stream-function/vorticity* form, thereby eliminating the pressure. The stream function Ψ and vorticity ζ are defined by

$$U = \frac{1}{r}\Psi_z, \quad W = -\frac{1}{r}\Psi_r, \quad \zeta = U_z - W_r,$$

and the problem to be solved transforms to

$$\nabla^2\Psi - \frac{2}{r}\Psi_r = r\zeta, \quad (2.10)$$

$$\text{Re} \left(-\frac{\zeta}{r^2}\Psi_z + \frac{1}{r}\Psi_z\zeta_r - \frac{1}{r}\Psi_r\zeta_z \right) = \nabla^2\zeta - \frac{\zeta}{r^2} - \frac{\text{Gr}}{\text{Re}}\Theta_r, \quad (2.11)$$

$$\text{Ma} \left(\frac{1}{r}\Psi_z\Theta_r - \frac{1}{r}\Psi_r\Theta_z \right) = \nabla^2\Theta, \quad (2.12)$$

with boundary conditions

$$\Psi = 0, \quad \zeta = \frac{1}{r}\Psi_{zz}, \quad \Theta = \mp\frac{1}{2}; \quad z = 0, \Gamma, \quad (2.13)$$

$$\Psi = \zeta = \Theta_r = 0; \quad r = 0, \quad (2.14)$$

$$\Psi = 0, \quad \zeta = \Theta_z, \quad \Theta_r = \text{Bi}[\Theta - \Theta_a(z)]; \quad r = 1. \quad (2.15)$$

These equations are solved using a modification of the predictor-corrector multiple iteration technique employed successfully by Neitzel [18] to study centrifugally unstable flows in cylindrical geometries. For results of the basic state computations and comments, we refer to [26].

3 Energy-stability analysis

We begin the energy-theory analysis of the basic state in the usual fashion, by deriving the energy identity. We assume there exists a solution $[\mathbf{u}, p, T]$ to the governing equations (equation (2.1)), plus the unsteady analogs of (2.2)–(2.5), which is a perturbation to the axisymmetric basic state, i.e.,

$$[\mathbf{u}, p, T] = [U(r, z), 0, W(r, z), P(r, z), \Theta(r, z)] \\ + [u'(r, \theta, z, t), v'(r, \theta, z, t), w'(r, \theta, z, t), p'(r, \theta, z, t), T'(r, \theta, z, t)]. \quad (3.1)$$

Substitution of (3.1) into the governing equations and boundary conditions leads to a system of equations for the disturbance quantities. We then take the inner product of the disturbance momentum equation with \mathbf{u}' , add to this the disturbance energy equation multiplied by $\lambda\text{Pr}T'$, and integrate over the volume

$$V = \{(r, \theta, z) \mid 0 \leq r \leq 1, 0 \leq \theta \leq 2\pi, 0 \leq z \leq \Gamma\}$$

occupied by the liquid, using the disturbance boundary conditions. The result is the exact disturbance-energy evolution equation

$$\frac{dE}{dt} = -\text{Pr}D - \text{Ma}I + \text{Pr}J, \quad E = \frac{1}{2} \int_V (\mathbf{u}' \cdot \mathbf{u}' + \lambda\text{Pr}T'^2) dV, \quad (3.2)$$

where

$$I = \int_V \left(\mathbf{u}' \cdot \mathbf{D} \cdot \mathbf{u}' + \lambda\text{Pr}T' \nabla \Theta \cdot \mathbf{u}' - \frac{\text{Gr}}{\text{Re}^2} w' T' \right) dV, \\ D = \int_V (\nabla \mathbf{u}' : \nabla \mathbf{u}' + \lambda \nabla T' \cdot \nabla T') dV, \quad J = \int_S (-w' T'_z + \lambda \text{Bi} T'^2) dS$$

and S is the free surface $r = 1$. The velocity and temperature disturbances have been joined by a positive *coupling parameter* λ [10] to form a generalized disturbance energy, E , and the quantity \mathbf{D} in the production integral I is the *symmetric* basic-state deformation-rate tensor,

$$\mathbf{D} = \begin{bmatrix} U_r & 0 & \frac{1}{2}(U_z + W_r) \\ & \frac{U}{r} & 0 \\ & & W_z \end{bmatrix}.$$

Employing the reformulated energy theory of Davis and von Kerczek [5], equation (3.2) is divided by the positive-definite functional E and an upper bound is constructed for the resulting right-hand side, viz.,

$$\frac{1}{E} \frac{dE}{dt} \leq \nu = \max_H \left(\frac{-\text{Pr}D - \text{Ma}I + \text{Pr}J}{E} \right), \quad (3.3)$$

where the maximum is taken over the space of kinematically admissible functions,

$$H = \{\mathbf{u}', T' \mid \mathbf{u}' = T' = 0 \text{ at } z = 0, \Gamma; u' = 0 \text{ at } r = 0, 1; \nabla \cdot \mathbf{u}' = 0\}.$$

We choose to formulate the problem so that the Reynolds number is the stability parameter. For fixed values of the other parameters associated with the problem, the smallest value of Re which corresponds to the condition $\nu = 0$ will be called $\text{Re}^*(\lambda)$.

The cylindrical geometry allows a Fourier decomposition in the azimuthal coordinate of the form

$$u'(r, \theta, z, t) \longrightarrow u(r, z, t)e^{in\theta} + u^*(r, z, t)e^{-in\theta},$$

where n is the azimuthal (integer) wavenumber and $*$ denotes complex conjugation.

Since λ is a free parameter, the maximum value of Re^* for positive values of λ is sought [10], while a minimization has to be carried out with respect to n . The resulting value is the energy-stability limit, Re_E , defined as

$$\text{Re}_E = \min_n \max_{\lambda > 0} \text{Re}^*. \quad (3.4)$$

In many analyses, the search for this maximum is not performed. Rather, the variable λ is arbitrarily set to some value, say $\lambda = 1$, and the result is accepted as a lower bound to the actual energy-stability limit. It will be seen that, for the problem of interest here, the effort necessary to determine Re_E is extremely worthwhile.

Typically, Re^* is calculated by treating the Euler-Lagrange system which arises from the maximum problem in (3.3). However, the basic state, which appears in the coefficients of these equations, is known only numerically. Thus, we choose to approach the calculation of Re^* by directly treating the functional ν in 3.3. It is convenient to consider a slightly different functional which incorporates the divergence constraint by means of a Lagrange multiplier. Hence, the maximum problem to be solved is expressed as

$$\max_h [\text{Pr}(-D - \text{Re}I + J) + 2 \int_V \pi \nabla \cdot \mathbf{u}' dV + \bar{\nu}(E - 1)] = 0, \quad (3.5)$$

where $\bar{\nu}$ is a Lagrange multiplier expressing the arbitrary normalization $E = 1$, $\pi(r, z)$ is a Lagrange multiplier, and h is the extension of H obtained by removing the divergence constraint. It is easy to show that $\bar{\nu} = \nu$. Thus, since the stability condition is given by $\nu = 0$, we are interested in the variation of the quadratic functional

$$F = \text{Pr}(-D - \text{Re}I + J) + 2 \int_V \pi \nabla \cdot \mathbf{u}' dV. \quad (3.6)$$

A discrete version of this functional follows in an obvious way. A grid system, which divides the flow region into N rectangular subdomains, is chosen. The *unknown* values of the disturbance velocity and temperature at the intersections of the grid are denoted by $u_{i,j}$, $v_{i,j}$, $w_{i,j}$ and $T_{i,j}$. Since the Lagrange multiplier π plays the same role as the fluid pressure, a staggered grid is employed for it; the

unknown values of π at the intersections of its grid are denoted by $\pi_{k,l}$. The various derivatives in the integrals of F are replaced by finite differences. The integrals are approximated on each subdomain by finite summations using the disturbance boundary conditions, where applicable, and finally the discrete version of the functional, F_D , is formed by summing over all N subdomains. We refer to [26], where details are given in the two-dimensional case, and to the appendix in [20].

A stationary value of F_D is located by differentiating it with respect to each unknown and setting each of these derivatives to zero, i.e.,

$$\frac{\partial F_D}{\partial q_n} = 0, \quad q_n = u_{i,j}, v_{i,j}, w_{i,j}, \phi_{i,j} \quad \text{or} \quad \pi_{k,l}. \quad (3.7)$$

This process yields a generalized algebraic eigenvalue problem. We seek the minimum positive eigenvalue of this system as the approximate (subject to discretization error) value of Re^* . Calling the vector consisting of the unknowns on all grid points \mathbf{X} , we rewrite (3.7) in the matrix form

$$\mathbf{A}\mathbf{X} = \rho\mathbf{B}(\text{Re})\mathbf{X}, \quad (3.8)$$

where \mathbf{A} and \mathbf{B} are *indefinite, Hermitian* matrices with \mathbf{A} having a banded structure and \mathbf{B} depending on the basic-state deformation-rate tensor \mathbf{D} . The fact that the matrices are Hermitian is due to the derivation from the variational problem (3.5). The dependence on the basic state, which depends in turn on the Reynolds number Re , complicates the calculation of Re^* . For a given value of Re , denote the smallest positive eigenvalue of the generalized eigenvalue problem (3.8) by ρ^* . If $\rho^* \neq \text{Re}$, then a new Re is chosen, the basic state recomputed, and the eigenvalues recalculated. This process is repeated until $\rho^* = \text{Re}$, in which case, $\text{Re}^* = \rho^*$. This, of course, assumes all other parameters, including the coupling parameter λ , are fixed, necessitating further computation to find Re_E according to (3.4).

4 Linear-stability analysis

The stability analysis of the basic-state velocity, $U(x)$, temperature, $T(x)$, and pressure, $P(x)$, fields begins in the usual fashion by assuming there exists a solution to the Boussinesq equations of the form

$$q(x, t) = Q(x) + q'(x, t)$$

where q refers to any flow quantity (i.e., velocity, temperature or pressure), a capital letter denotes the basic state and a prime is used to denote a disturbance. Substitution of the solution into the Boussinesq equations and linearization in disturbance quantities leads to the *linearized disturbance equations* (dropping primes):

$$\text{Re}[u_t + Uu_r + uU_r + Wu_z + wU_z] = -p_r + \left[\frac{1}{r}(ru)_r \right]_r + \frac{1}{r^2}u_{\varphi\varphi} + u_{zz} - \frac{2}{r^2}v_{\varphi}, \quad (4.1)$$

$$\text{Re} \left[v_t + Uv_r + Wv_z + \frac{Uv}{r} \right] = -\frac{1}{r}p_{\varphi} + \left[\frac{1}{r}(rv)_r \right]_r + \frac{1}{r^2}v_{\varphi\varphi} + v_{zz} + \frac{2}{r^2}u_{\varphi}, \quad (4.2)$$

$$\text{Re}[w_t + Uw_r + uW_r + Ww_z + wW_z] = -p_z + \frac{\text{Gr}}{\text{Re}}\theta + \left[\frac{1}{r}(rw)_r \right]_r + \frac{1}{r^2}w_{\varphi\varphi} + w_{zz}, \quad (4.3)$$

$$\text{Ma}[\theta_t + U\theta_r + uT_r + W\theta_z + wT_z] = \frac{1}{r}[r\theta_r]_r + \frac{1}{r^2}\theta_{\varphi\varphi} + \theta_{zz} \quad (4.4)$$

$$(ru)_r + v_{\varphi} + (rw)_z = 0. \quad (4.5)$$

In equations (4.1)–(4.5) we have scaled velocities by $\gamma\Delta T/\mu$, pressure by $\gamma\Delta T/R$, temperature by ΔT , and time by $R\mu/(\gamma\Delta T)$, where $\Delta T = T_H - T_C$, γ is the (positive) rate of decrease of surface tension with respect to temperature, and μ is the coefficient of dynamic viscosity of the liquid in the zone. The disturbance temperature is denoted by θ .

The boundary conditions which complete the specification of the problem are

$$u = v = w = \theta = 0, \quad z = 0, \Gamma, \quad (4.6)$$

$$u = w_r + \theta_z = v_r - v/r + \theta_\varphi = \theta_r + \text{Bi}\theta = 0, \quad r = 1, \quad (4.7)$$

in addition to the requirement that all flow quantities remain bounded at $r = 0$.

In view of the linearity of (4.1)–(4.5) and the fact that the coefficients depend only on r and z , we make use of Floquet theory and normal modes to write all flow quantities as

$$q(r, \varphi, z, t) = q^*(r, z) \exp(\sigma t + im\varphi) \quad (4.8)$$

where $\sigma = \sigma_R + i\sigma_I$ is the complex growth rate and m is restricted to be an integer. Again, we refer to [9] for more details. Marginal stability corresponds to the condition $\sigma_R = 0$. The form (4.8) is now substituted into (4.1)–(4.5) and the boundary conditions. A discrete version of the resulting problem is a complex, generalized eigenvalue problem of the form

$$Ax = \sigma Bx, \quad (4.9)$$

where x is the vector of unknown velocity, temperature and pressure values at the nodes of the appropriate grid.

The corresponding eigenvalue problem from the energy-theory analysis of this basic state was, at worst, complex-Hermitian (in addition to being indefinite and sparse), whereas (4.9) has no such symmetry. An additional complication, which also existed as part of the energy-stability analysis, is the fact that the basic-state velocity and temperature fields depend upon the stability parameter, Ma (equivalently, Re). For the energy-theory calculations, this required an additional level of iteration to obtain the energy limit, Ma_E . Since we formulate the problem with σ as the eigenvalue, our procedure is to fix the Prandtl, Grashof and Biot numbers as well as the azimuthal wavenumber m and calculate the eigenvalue of system (4.9) with largest *real* part, call it σ^* , for various values of the Marangoni number. The Marangoni number Ma^* corresponding to $\sigma_R^* = 0$ is the value above which infinitesimal disturbances of azimuthal wavenumber m will grow. The linear-stability limit, $\text{Ma}_L(\text{Pr}, \text{Gr}, \text{Bi})$, is therefore given by

$$\text{Ma}_L(\text{Pr}, \text{Gr}, \text{Bi}) = \min_m \text{Ma}^*(\text{Pr}, \text{Gr}, \text{Bi}; m). \quad (4.10)$$

5 The numerical method-energy stability

Equation (3.8) represents a nonlinear generalized eigenvalue problem. The matrices \mathbf{A} and \mathbf{B} are symmetric and sparse, but, in general, indefinite. In addition to the basic-state dependence of \mathbf{B} mentioned above, \mathbf{A} and \mathbf{B} depend on the other parameters of the problem, namely, Pr , Gr and the coupling parameter, λ . We first address the case that all these parameters are fixed, reducing (3.8) to the generalized eigenvalue problem

$$\mathbf{A}\mathbf{X} = \rho\mathbf{B}\mathbf{X}, \quad \|\mathbf{X}\| = 1, \quad (5.1)$$

where $\|\cdot\|$ denotes the Euclidean norm.

The eigenvalues ρ of (5.1) may be real of either sign or be complex-conjugate pairs. To each null vector of \mathbf{B} corresponds an “infinite” eigenvalue (at least N of these are known to occur), while the null vectors of \mathbf{A} yield zero eigenvalues. Standard linear-algebra software packages provide implementations of the *QZ*-algorithm for eigenvalue problems of the form (5.1). These packages compute *all* of the eigenvalues of the system (our stability result requires only a *single* eigenvalue), do not exploit the sparseness of \mathbf{A} and \mathbf{B} and are therefore suitable only for relatively coarse discretizations of the underlying continuous problem. The method adopted for the present computations makes use of both the symmetry and sparseness of \mathbf{A} and \mathbf{B} and computes only the eigenvalue of interest—the smallest, positive one.

The algorithm of choice for finding a single eigenvalue of (5.1) appears to be some form of *inverse iteration*. The technique used here is a generalization of that employed by [2] in the program PLTMG for the simpler problem of finding the smallest eigenvalue of a positive-definite matrix. For this a starting vector \mathbf{X}_0 , $\|\mathbf{X}_0\| = 1$, is needed. Initially, this inverse iteration process is started with a random vector. Subsequent iterations use previously computed eigenvectors corresponding to nearby parameter values. A first approximation for ρ is obtained through the *Rayleigh quotient*

$$\rho_0 = \mathbf{X}_0^T \mathbf{A} \mathbf{X}_0 / \mathbf{X}_0^T \mathbf{B} \mathbf{X}_0. \quad (5.2)$$

In the unlikely event that the denominator is zero, a different \mathbf{X}_0 has to be chosen.

Given this initial pair \mathbf{X}_0 and ρ_0 , the inverse iteration procedure is performed as follows:

1. Solve $(\mathbf{A} - s\mathbf{B})\bar{\mathbf{Y}} = (\rho_k \mathbf{B} - \mathbf{A})\mathbf{X}_k$ and define $\mathbf{Y} = \frac{\bar{\mathbf{Y}} - \bar{\mathbf{Y}}^T \mathbf{X}_k}{\|\bar{\mathbf{Y}} - \bar{\mathbf{Y}}^T \mathbf{X}_k\|}$.
2. Form $\mathbf{Q} = [\mathbf{X}_k | \mathbf{Y}]$ and solve the 2×2 problem

$$\mathbf{Q}^T \mathbf{A} \mathbf{Q} \mathbf{Z} = \tau \mathbf{Q}^T \mathbf{B} \mathbf{Q} \mathbf{Z}$$

for the eigenvalues τ_1, τ_2 and associated normalized eigenvectors $\mathbf{Z}_1, \mathbf{Z}_2$. Without loss of generality let τ_1 be the *smallest positive* eigenvalue.

3. Set $\rho_{k+1} = \tau_1$, $\mathbf{X}_{k+1} = \mathbf{Q} \mathbf{Z}_1$ and check for convergence. If not converged, increment iteration index k and repeat.

Several remarks are in order on the above algorithm. The quantity s is a positive real number which has to be closer to the desired eigenvalue than to any of the other eigenvalues. While, in some applications this “shift parameter” may have to be adjusted during the computation in order to satisfy this requirement, this was not necessary in the present case. Earlier computations with the QZ -algorithm for moderate-size problems had shown that, for the cases considered, there were no complex-conjugate pairs that were smaller in modulus than ρ^* . Also, the negative eigenvalue of smallest modulus was similar in modulus to ρ^* . It was thus relatively easy, with some rough knowledge of ρ^* , to find a value for s .

The eigenvalue problem in step 2 is basically an orthogonal projection of the original problem into the subspace spanned by the columns of \mathbf{Q}_k . Simpler inverse iteration algorithms are indeed available; however, their application to the present problem did not yield satisfactory results. In general, of course, this 2×2 eigenvalue problem may have complex eigenvalues, as well as real ones. While several precautions for this and other cases were put into the program, they will not be described here, being a rather technical detail. Eventually τ_1 will be positive and approximate ρ^* while $\mathbf{Q} \mathbf{Z}_1$ approximates the associated eigenvector. \mathbf{X}_{k+1} and ρ_{k+1} are related through the Rayleigh quotient (5.2).

While steps 2 and 3 need no further explanation, the solution of the linear system in step 1 represents a nontrivial problem. The matrix on the left is symmetric but indefinite. The newest version of the FORTRAN subroutine SYMMLQ, part of the NAG library, was used. It applies a conjugate-gradient method and permits preconditioning by a positive-definite matrix. No attempt was made to find a near optimal choice for the preconditioner. In all computations it was taken as the diagonal matrix with the i -th element equal to the Euclidean norm of the i -th column of the matrix $\mathbf{A} - s\mathbf{B}$.

The convergence of the above inverse iteration procedure is linear with a factor asymptotically equal to

$$\left| \frac{s - \rho^*}{s - \rho_n} \right| < 1$$

where ρ_n is the next nearest eigenvalue of (5.1) to s . Choosing s close to ρ^* will thus speed up convergence of the inverse iteration while, in general, requiring more conjugate-gradient iterations for the nearly singular system matrix. The essential computational requirement per conjugate-gradient iteration is one matrix-vector multiplication with the system matrix.

In addition to this method for solving the eigenvalue problem, two outer iterations are needed to determine the energy-stability limit Ma_E . The requirement that $\rho^*(\text{Ma}) = \text{Ma}$ suggests a fixed-point iteration. The second requirement, that Ma_E is found as the maximum of all these ρ^* with respect to λ suggests an optimization procedure. No attempt was made to simultaneously attack both these problems. Both possibilities of a successive solution were used, the fixed-point iteration as either an inner or outer iteration. In the first case, say, when λ is temporarily fixed, the following would be the well-known Picard iteration

$$\mathbf{A}\mathbf{X}_{k+1} = \rho_{k+1}\mathbf{B}(\rho_k)\mathbf{X}_{k+1}, \quad k = 0, 1, 2, \dots \quad (5.3)$$

where $\rho_{k+1}, \mathbf{X}_{k+1}$ is the solution found through the inverse iteration procedure defined above. This iteration will only converge if $|\varphi'(\text{Ma}^*)| < 1$, where φ denotes the relationship between ρ_{k+1} and ρ_k given through (5.3) and if started close enough to Ma^* . A simple acceleration procedure due to [1] was implemented to guarantee convergence:

$$\begin{aligned} \rho_k^{(0)} &= \rho_k, \\ \rho_k^{(i)} &= \varphi(\rho_k^{(i-1)}), \quad i = 1, 2, \\ \rho_{k+1} &= \rho_k + \frac{(\rho_k^{(1)} - \rho_k^{(0)})^2}{(\rho_k^{(1)} - \rho_k^{(0)}) - (\rho_k^{(2)} - \rho_k^{(1)})}. \end{aligned} \quad (5.4)$$

The sequence $\{\rho_k\}$ converges quadratically if φ is twice continuously differentiable and $\varphi'(\text{Ma}^*) \neq 1$.

For the sake of completeness we also outline how the maximization of Ma^* with respect to λ was accomplished. Starting from an initial value λ_1 and corresponding value ρ_1 (or Ma_1) two additional pairs of values are computed with their λ -values in the vicinity of λ_1 . Through these 3 points a quadratic parabola is fit and the point corresponding to its maximum replaces one of the points. The parabola need not have a maximum; in the event that a minimum occurs, some modification is required. The details will again not be given here since they are straightforward. As is well known, maximization through successive quadratic interpolation has a convergence order of about 1.3.

The iterative procedure described above provides a relatively efficient method to calculate Ma_E . After computation of the first basic state, subsequent basic-state computations need fewer relaxations if they are done for a convergent sequence of Marangoni numbers. Analogously, the inverse iteration only requires several (more than 1-2) iterations when initiated, i.e., with the random vector \mathbf{X}_0 . It is thus not surprising that the entire computation of Ma_E took only a few times the amount of work needed for the first basic state and ρ^* -computation. It should be noted that, to minimize inaccuracies introduced by differentiation of basic-state quantities, the basic state was computed on a grid with *twice* the resolution used for the stability calculations.

6 The numerical method-linearized stability

As shown above, the determination of the linear stability bounds Ma_L requires the solution of the following eigenvalue problem

$$A\mathbf{x} = \sigma B\mathbf{x} \quad (6.1)$$

where A, B are $N \times N$ matrices, $N = k + l$, which are partitioned as

$$A = \begin{pmatrix} A_{11} & A_{12} \\ A_{21} & A_{22} \end{pmatrix}, \quad B = \begin{pmatrix} B_{11} & 0 \\ 0 & 0 \end{pmatrix} \quad (6.2)$$

$A_{11}, B_{11} \in C^{k,k}$, $A_{22} \in C^{l,l}$, where k is the number of velocity/temperature unknowns and l the number of pressure unknowns. The matrices are derived from linearizing the boundary value problem for the Boussinesq equations at the solution (basic state) for specific values of the parameters (Pr, Gr, Bi). A is complex and non-Hermitian while B_{11} is taken as a multiple of the identity matrix. If the real parts of all eigenvalues are negative, the basic state is stable, and for increasing Ma that value Ma^* has

to be found where for the first time an eigenvalue, to be called the critical eigenvalue in the following, crosses the imaginary axis. Here, it is expected that this corresponds to a simple Hopf bifurcation point [8]; that is, there will be exactly one complex-conjugate eigenvalue pair with nonzero imaginary part that crosses the imaginary axis with nonzero speed.

There is a sizable literature on the numerical computation of Hopf bifurcation points; instead of attempting to give a necessarily rather incomplete listing of works, we refer to a recent collection of articles on bifurcation problems [17] in which several papers address this issue.

Generalized eigenvalue problems of the form (6.1), on the other hand, particularly if they arise from applications as is the case here, have been studied thoroughly, and many contributions have been made to their numerical solution. Again, we confine references to just one recent survey work [11] which also includes an extensive bibliography.

Frequently, Hopf bifurcation points are detected during a continuation process. For this, in general, all eigenvalues of (6.1) are computed, a procedure that is prohibitively expensive for large problems ($N > 10^4$). After the detection of a Hopf point, its precise location may be determined through characterizing extended systems; see [27], [6] and the references therein. This technique has proven to be useful for problems of moderate size while it is of limited use for very large problems.

From the literature dealing with the computation of Hopf points in flow problems, [4] shall be quoted exemplarily. In this work, a relatively sophisticated combination of numerical techniques was applied to a nontrivial hydrodynamic stability problem. One feature common to the numerical approaches in [4] and many other works is the direct solution of the occurring linear systems of equations. This feature still limits the size of the problems. The dimensions of the eigenvalue problems solved are a few thousand. On the other hand, in [26] the iterative solution of these problems permitted (in-core) solution of problems of dimension $10^4 - 10^5$. From the experience with the related but different computations of the energy stability bounds in [26], there was reason to hope that, also for the determination of the linearized stability limits, a method of inverse iteration type would yield the desired results.

If it was known in advance with which imaginary part β the critical eigenvalue crosses the imaginary axis, then inverse iteration with shift $i\beta$ would allow detection of this Hopf point at least when the computation is started in the stable range, not too far from the critical parameter value and continuation in this parameter is employed. It is clear that, to safeguard the obtained results, computations must be done with different values of β . Alternatively, generalizations of the numerical algorithm, i.e., the Arnoldi method, must be used to compute more than one eigenvalue at a time as was done for medium-fine discretizations. On coarse meshes all eigenvalues could be computed using the QZ method. Then, Arnoldi [25] was used to compute 10–15 eigenvalues near that of largest real part. Roughly, the computational work was greater than that for the inverse iteration used subsequently by a factor equal to the number of eigenvalues computed.

Let s denote the shift that is usually anticipated to be purely imaginary with, say, positive imaginary part β . The following form of inverse iteration was successfully applied to the present problem.

$$(A - sB)\delta x_k = (\sigma_k B - A)x_k, \quad (6.3)$$

$$\begin{aligned} \sigma_{k+1} &= \frac{(x_k + \delta x_k)_i}{\sigma_k [x_k]_i}, \\ x_{k+1} &= \frac{x_k + \delta x_k}{[x_k + \delta x_k]_i}, \end{aligned}$$

where $[x]_i$ denotes the component of the largest modulus of a vector $x \in C^n$. Here, x_0 was initially, i.e., for the first Marangoni number used, chosen as a random vector and σ_0 as 1. For a fixed shift, convergence of both the eigenvalue and eigenvector approximations will in general be linear with a factor

$$\left| \frac{s - \sigma^*}{s - \sigma_n} \right| < 1 \quad (6.4)$$

where σ^* , σ_n are the nearest and the next nearest eigenvalue to s . Also, faster convergence for the σ_k could be obtained by iterating with approximate left eigenvectors and using the generalized Rayleigh quotient, cf; e.g., [11].

The essential computational work involved in the proposed method is the solution of the linear system in (6.3a). The matrix $C = A - sB$ is complex and non-Hermitian. First, an equivalent real system of order $2N$ was formed for the matrix

$$\overline{C} = \begin{pmatrix} \operatorname{Re}(C) & -\operatorname{Im}(C) \\ \operatorname{Im}(C) & \operatorname{Re}(C) \end{pmatrix}.$$

This system was then solved using the conjugate gradient method for the normal equations [22]. For this the matrix \overline{C} was first scaled by multiplying the matrices A_{ij} in (6.2) with appropriate powers of the discretization parameters to balance \overline{C} . Then, additionally, a diagonal scaling was used such that the columns of \overline{C} had unit norm. Different preconditionings may well lead to a more efficient solution method; several, however, were tried without yielding a substantial reduction in work. These included outer-inner iterations utilizing the partitioning in (6.2) as, for example, in [3] for the Stokes problem. Here, however, $A_{11} - sB_{11}$ is neither Hermitian nor definite. An incomplete LU decomposition was used to precondition the inner iterations. Nevertheless, a higher efficiency is to be expected from an adaptive multilevel approach such as hierarchical bases [3]. Instead, the finite difference discretization given above was used on a fixed grid so that the results could be compared to the energy stability results of [20], where the analogous discretization was used. Studies with various grid sizes suggest that the error of the numerical results is well below 1%.

Instead of the normal equations, the system with \overline{C} could have been solved directly by suitable generalizations of conjugate gradients, such as biconjugate gradients, biconjugate gradients squared, generalized minimal residuals, etc. No preconditioners could easily be found that made these methods sufficiently efficient for the cases to be solved. While \overline{C} will not generally be exactly singular if $i\beta \neq \operatorname{Im}(\sigma^*)$, it will be nearly singular. It must also be noted that the values of $\operatorname{Im}(\sigma^*)$ were in the range $10^{-2} - 10^{-1}$.

7 An exemplary numerical result

For detailed numerical results and discussion, we refer to our papers quoted below; similarly for details on the experiences with the numerical procedures outlined above. However, at least one typical result will be presented together with comparison values obtained in the literature.

We consider the problem with $\operatorname{Gr} = 0$, $\operatorname{Bi} = 0$, $\operatorname{Pr} = 1$, $\Gamma = 1.2$. For this case, according to numerical results reported in [24] a three-dimensional simulation of the nonlinear flow problem yields an onset of instability at the (rescaled) Marangoni number of 2250. Experimental results in [28] indicated this value to be about 1030, while our energy and linearized analyses resulted in Ma_E around 1400 [20] and $\operatorname{Ma}_L = 1820$ [19]. For a discussion of the possible reasons for the discrepancies in these bounds we again refer to the literature quoted.

References

- [1] Aitken, A. C., *On Bernoulli's numerical solution of algebraic equations*, Proc. Roy. Soc. Edinburgh **46**, 289.
- [2] Bank, R. and Mittelmann, H. D., *Continuation and multigrid for nonlinear elliptic systems*, Lecture Notes in Mathematics 1228, *Multigrid Methods II*, Hackbusch, W. and Trottenberg, U., eds., Springer-Verlag, Berlin, New York (1986).
- [3] Bank, R. E., Welfert, B. D. and Yserentant, H., *A class of iterative methods for solving saddle point problems*, Numer. Math. **56** (1990), 645–666.

- [4] Christodoulou, K. N. and Scriven, L. E., *Finding leading modes of a viscous free surface flow: An asymmetric generalized eigenproblem*, J. Sci. Comput. **3** (1988), 355–405.
- [5] Davis, S. H. and von Kerczek, C., *A reformulation of energy stability theory*, Arch. Rat. Mech. Anal. **52** (1973), 112–117.
- [6] Dedier, B., Roose, D. and Van Rompay, P., *Interaction between fold and Hopf curves leads to new bifurcation phenomena*, in *Continuation Techniques and Bifurcation Problems*, Mittelmann, H. D. and Roose, D., eds., 171–186 (1990).
- [7] Eyer, A., Leiste, H. and Nitsche, R., *Floating zone growth of silicon under microgravity in a sounding rocket*, J. Crystal Growth **71** (1985), 173–182.
- [8] Hopf, E., *Abzweigung einer periodischen Lösung von einer stationären Lösung eines Differential-systems*, Ber. Verh. Sachs. Akad. Wiss. Leipzig. Math.-Nat. K1.95 **1** (1943), 3–22.
- [9] Ioss, G. and Joseph, D. D., *Elementary Stability and Bifurcation Theory*, Springer-Verlag, New York, Berlin, Heidelberg, 1990.
- [10] Joseph, D. D., *Stability of Fluid Motions I, II*, Springer-Verlag, Berlin, (1976).
- [11] Kerner, W., *Large-scale complex eigenvalue problems*, J. Comput. Phys. **85** (1989), 1–85.
- [12] Kuhlmann, H. C., *Thermocapillary Flows in Finite Size Systems*, Math. Comput. Modelling **20** (1994), 145–173.
- [13] Levenstam, M. and Amberg, G., *Hydrodynamic instabilities of thermocapillary flow in a half-zone*, J. Fluid Mech. **297** (1995), 357–372.
- [14] Mittelmann, H. D., *Hydrodynamic stability of thermocapillary convection in liquid bridges*, Math. Comput. Modelling **20** (1994), pp. 178–188.
- [15] Mittelmann, H. D., Chang, K.-T., Jankowski, D. F. and Neitzel, G. P., *Iterative solution of the eigenvalue problem in Hopf bifurcation for the Boussinesq equations*, SIAM J. Comp. **15** (1994), 704–712.
- [16] Mittelmann, H. D., Law, C. C., Jankowski, D. F. and Neitzel, G. P., *A large, sparse, and indefinite generalized eigenvalue problem from fluid mechanics*, SIAM J. Sci. Stat. Comp. **13** (1992), 411–424.
- [17] Mittelmann, H. D. and Roose, D., eds., *Continuation Techniques and Bifurcation Problems*, ISNM 92, Birkhäuser-Verlag, Basel, 1990.
- [18] Neitzel, G. P., *Numerical computation of time-dependent Taylor-vortex flows in finite-length geometries*, J. Fluid Mech. **141** (1984), 51–66.
- [19] Neitzel, G. P., Chang, K.-T., Jankowski, D. F. and Mittelmann, H. D., *Linear-stability theory of thermocapillary convection in a model of the float-zone crystal-growth process*, Phys. Fluids A **5** (1993), 108–114.
- [20] Neitzel, G. P., Law, C. C., Jankowski, D. F. and Mittelmann, H. D., *Energy stability of thermocapillary convection in a model of the float-zone crystal-growth process. Part 2, Non-axisymmetric disturbances*, Phys. Fluids A **3** (1991), 2841–2846.
- [21] Paige, C. C. and Saunders, M. A., *Solution of sparse indefinite systems of linear equations*, SIAM J. Numer. Anal. **12** (1975), 617–629.
- [22] Paige, C. C. and Saunders, M. A., *LSQR: An algorithm for sparse linear equations and sparse least squares*, ACM Trans. Math. Software **8** (1982), 43–71.

- [23] Preisser, F., Schwabe, P. and Scharmann, A., *Steady and oscillatory thermocapillary convection in liquid columns with free cylindrical surface*, J. Fluid Mech. **126** (1983), 545–567.
- [24] Rupp, R., Müller, G. and Neumann, G., *Three-dimensional time dependent modelling of the Marangoni convection in zone melting configurations for GaAs*, J. Crystal Growth **97** (1989), 34–41.
- [25] Saad, Y., *Variations of Arnoldi's method for computing eigenvalues of large unsymmetric matrices*, Linear Algebra Appl. **34** (1980), 269–295.
- [26] Shen, Y., Neitzel, G. P., Jankowski, D. F., and Mittelman, H. D., *Energy stability of thermocapillary convection in a model of the float-zone crystal-growth process*, J. Fluid Mech. **217** (1990), 639–660.
- [27] Spence, A., Cliffe, K. A. and Jepson, A. D., *A note on the calculation of paths of Hopf bifurcations*, in *Continuation Techniques and Bifurcation Problems*, Mittelman, H. D. and Roose, D., eds., 125–131 (1990).
- [28] Velten, R., Schwabe, D., and Scharmann, A., *The periodic instability of thermocapillary convection in cylindrical liquid bridges*, Phys. Fluids A **3** (1991), 267–279.
- [29] Xu, J.-J. and Davis, S. H., *Convective thermocapillary instabilities in liquid bridges*, Phys. Fluids **27** (1984), 1102–1107.